Structural Engineering and Mechanics, *Vol. 48, No. 4 (2013) 569-585*
DOI: http://dx.doi.org/10.12989/sem.2013.48.4.569

Impact of a shock wave on a structure strengthened by rigid polyurethane foam

Sherif A. Mazek[*1] and Ashraf A. Mostafa[2a]

[1]*Civil Engineering Department, Military Technical College, Kobbry El-Kobba, Khlifa El-Maamoon, Cairo, Egypt*
[2]*Egyptian Engineering Department, Cairo, Egypt*

(Received September 4, 2013, Revised October 28, 2013, Accepted October 29, 2013)

Abstract. The use of the rigid polyurethane foam (RPF) to strengthen sandwich structures against blast terror has great interests from engineering experts in structural retrofitting. The aim of this study is to use the RPF to strengthen sandwich steel structure under blast load. The sandwich steel structure is assembled to study the RPF as structural retrofitting. The filed blast test is conducted. The finite element analysis (FEA) is also used to model the sandwich steel structure under shock wave.
The sandwich steel structure performance is studied based on detonating different TNT explosive charges. There is a good agreement between the results obtained by both the field blast test and the numerical model. The RPF improves the sandwich steel structure performance under the blast wave propagation.

Keywords: displacements; field blast test; finite element analysis; blast wave; sandwich steel structure; TNT explosive charge

1. Introduction

The number of explosive attacks on civilian structure has recently increased worldwide. Protection of structure subjected to blast load remains quite sophisticated to predict. Current codes and regulations to estimate blast stress wave intensities effect on structures are usually based on some empirical methods due to the extreme complexities of the phenomenon of the blast process (Aimone 1982, Liu and Katsabanis 1997, Fayad 2009, Mohamad 2006, Schueller 1991, Zhang and Valliappan 1990). These empirical methods were obtained from observations and measurements in field blast tests. The empirical methods tended to overlook the physical laws governing the blast process (Beshara 1994, Smith and Hetherington 1994). Different countries and group of countries apply different design manuals (Remennikov 2003, Gustafsson 1973, Liu and Katsabanis 1997, Technical Manual TM 5-885-1 1986, Technical Manual TM 5-1300 2008).

It is very expensive to conduct field blast tests in every site and sometimes it is impossible to carry out such field tests due to safety and environmental constraints (Dharmasena *et al*. 2008, Hao *et al*. 1998). However, a reliable numerical model validated against measured field data is an effective tool to analyze the structure performance under blast effect (Chen and Chen 1996,

∗Corresponding author, Professor, E-mail: samazek@yahoo.com
[a]E-mail: agwa100@gmail.com

http://www.techno-press.org/?journal=sem&subpage=8 ISSN: 1225-4568 (Print), 1598-6217 (Online)

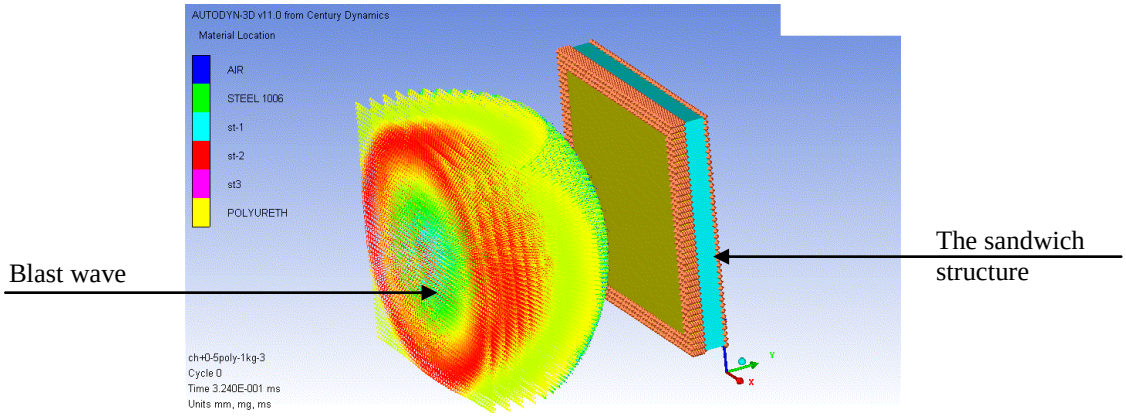

Fig. 1 Blast wave propagation hitting sandwich steel structure using 3-D numerical model

Dharmasena *et al*. 2008, Hao *et al*. 1998). Lu *et al*. (2005) used a fully coupled numerical model to simulate the response of buried concrete structure under subsurface blast. The responses of the buried structure obtained by 2-D numerical model at different points were compared by those obtained by 3-D numerical model. Trelat *et al*. (2007) studied impact of shock wave on structure due to explosion at altitude. They improved the understanding of interaction of blast waves with both ground and structure using both the FEA and the experimental work. Luccioni *et al*. (2009) studied craters produced by underground explosions. They discussed the accuracy of numerical simulation of craters produced by underground explosions. Ha *et al*. (2011) used carbon fibber reinforced polymer (CFRP) to strengthen structures against blast load. They conducted an experimental work on CFRP to strengthen RC panels under blast loading.

In this study, the field blast test is conducted to record pressure-time history of blast load hitting the steel structure and to record maximum displacement at the centre point of the sandwich steel structure. 3-D FEA is used to study the performance of the sandwich steel structure under blast effect. Based on the FEA, the performance sandwich steel structure strengthened by the rigid polyurethane foam (RPF) is studied. The RPF is considered as a mitigation system to strengthen sandwich steel structure against blast impact. Developing such a numerical method has always been a challenge due to the complicated properties of blasting process and highly nonlinear and strain rate dependent dynamic responses (Hao *et al*. 1998, Smith and Hetherington 1994). The pressure-time histories calculated by the numerical model are compared with those obtained by the field blast test and the empirical method.

Fireball and blast wave can travel in free air to hit the sandwich steel structure, as shown in Fig. 1. In this study, the performance of the sandwich steel structure with the different internal core structure systems is studied with and without using the RPF. In this study, hexagonal core sandwich steel structure (XCS) and channel stiffener sandwich steel structure (CSS) are prepared and assembled to discuss the effect of the RPF layer covering the front face of the steel structure, as shown in Figs. 2 and 3. The XCS and the CSS structures are the most famous sandwich steel doors used to protect civilian structures (Fayad 2009, Mohamad 2006, Baker *et al*. 1983, Wu *et al*. 1999).

The pressure-time histories hitting the sandwich steel structure are calculated by the both the empirical method developed by Henrych (Beshara 1994) and the numerical model. This study is also extended to compare the pressure-time histories obtained by the field blast test, the empirical

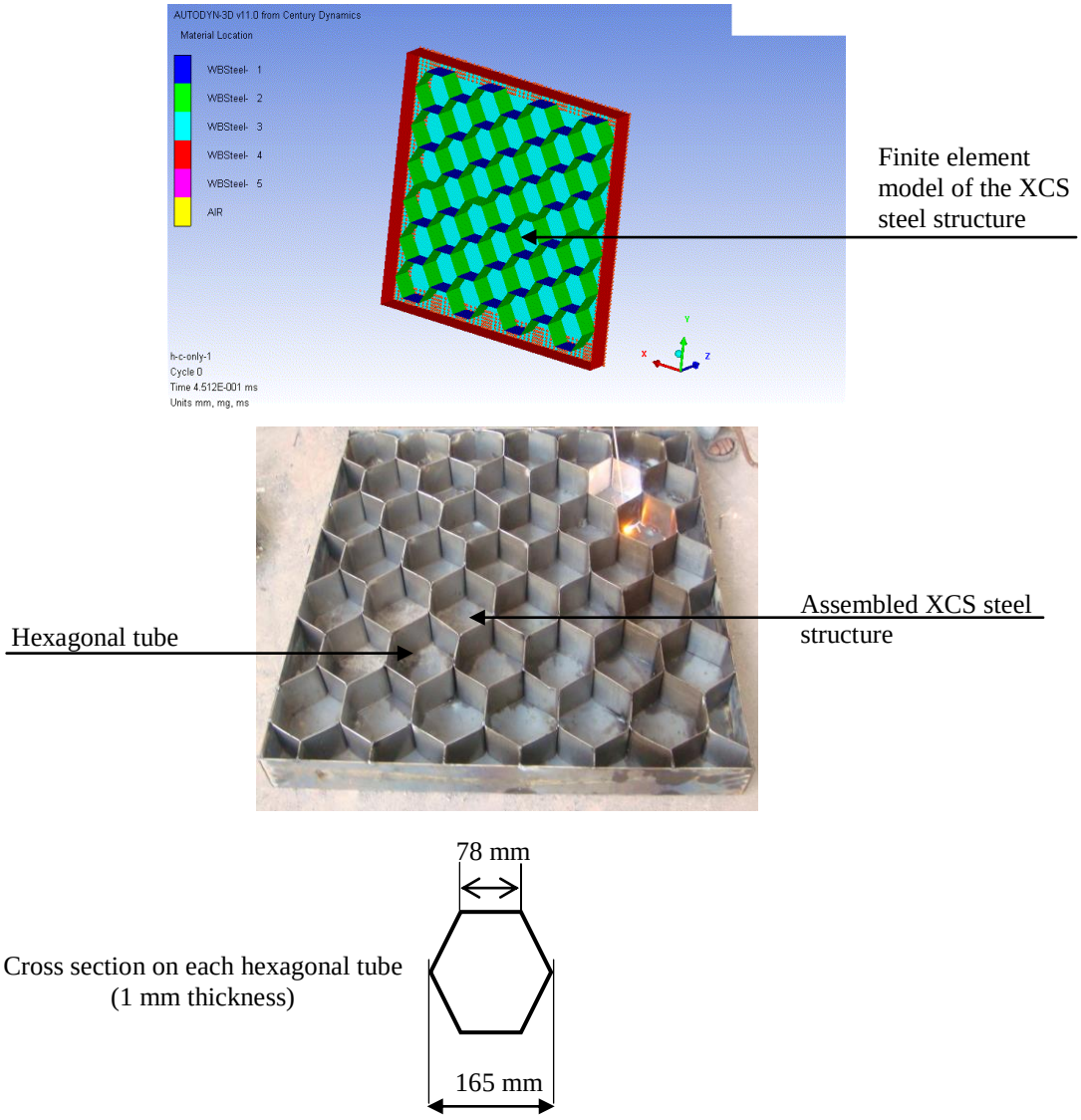

Fig. 2 Assembled hexagonal core sandwich steel structure (XCS) (hexagonal tube)

method, and the numerical model. The FEA is used to study the performance of the sandwich steel structure strengthened by the RPF. The constitutive model for this analysis contains elasto-plastic materials. An elasto-plastic model is also employed to represent the sandwich steel structure and the RPF layer.

The sandwich steel structure model strengthened by the RPF is implemented in a finite element code Autodyn3D (2005). Numerical results obtained by the FEA are compared with the data obtained from the field data. It shows that the numerical model can well predict the pressure-time hitting the steel structures. Maximum displacement-time histories of sandwich steel structure strengthened by the RPF are calculated and presented. The study shows the impact of the RPF on the performance of the sandwich steel structures.

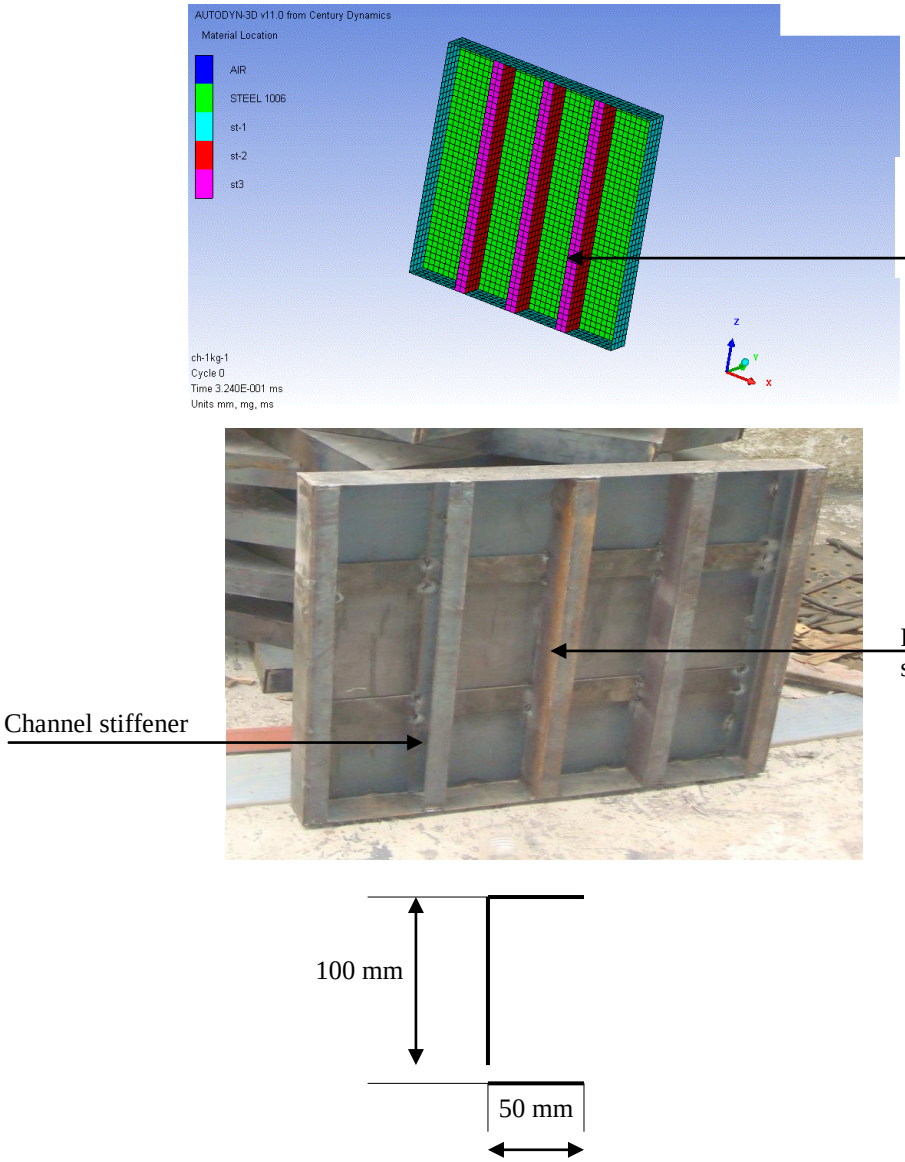

Cross section on each channel stiffener
(2 mm thickness)

Fig. 3 Assembled channel stiffener sandwich steel structure (CSS)

2. Numerical model

In numerical modeling, air and equivalent TNT explosive are simulated by Euler processor, as shown in Fig. 1. The air and the equivalent TNT explosive are assumed to satisfy the equation of state (EOS) of ideal gas (Hao *et al*. 1998). The sandwich steel structure and the RPF layer are modeled by the modified isotropic damage model and simulated by Lagrange processor (Hao *et al*.

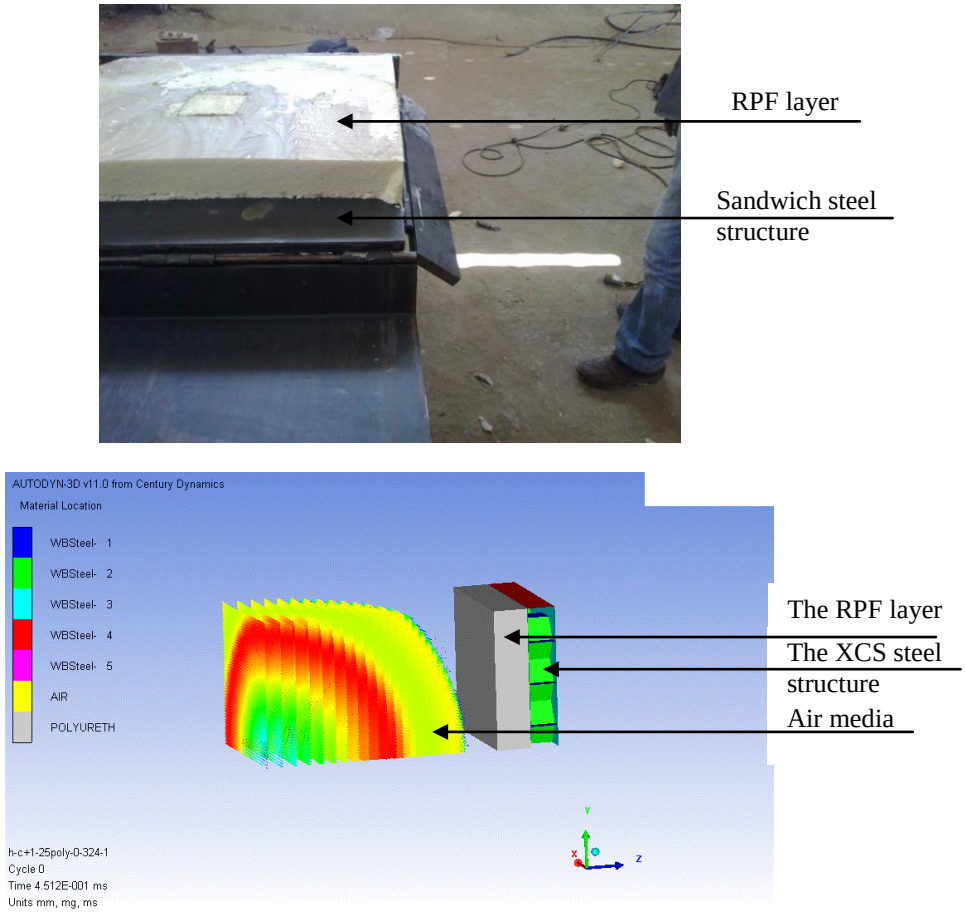

Fig. 4 3-D finite element model of the sandwich steel structure strengthened by RPF layer

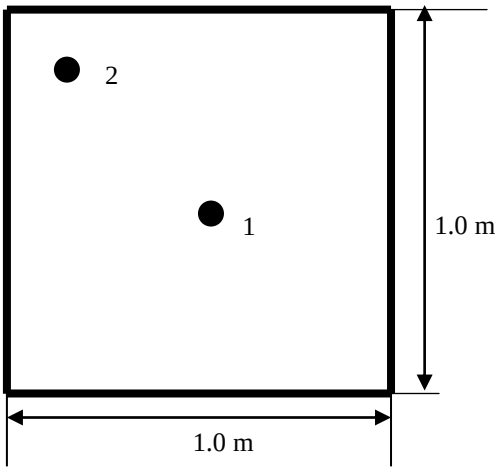

Fig. 5 Position of sensor located at the sandwich steel panel for points 1 and 2 (Field test and numerical model)

1998, Wu *et al*. 1999), as shown in Fig. 4. The whole domain, including the air media, the RPF layer, the sandwich steel structure, and the TNT explosive, is assumed to be symmetric in the *X*, *Y*, *Z* directions, as shown in Figs. 4 and 5. Transmitting boundary is used to reduce reflection of stress wave from the numerical boundaries. The standard constants of air, TNT explosive, and RPF layer are obtained from the Autodyn3D material library. These include air initial internal energy E_n=2.068×10^5 kJ/kg; air mass density ρ=1.225 kg/m^3; and ideal air constant γ=1.4. It should also be noted that viscous damping effect is neglected in the numerical simulation as its influence on high velocity explosion-type responses is insignificant (Hao *et al*. 1998, Wu *et al*. 1999).

Shell element is used to model both the membrane (in-plane) and the bending (out-of-plane) behavior of the sandwich steel structure including the internal core structure system, as shown in Figs. 2 to 4. In this study, the civilian structure including the sandwich steel structure with and without the RPF layer is modeled. The boundary condition applied to the sandwich steel structure is defined as hinged supports, as shown in Fig. 5. The dimensions of the sandwich steel structure are also shown in Fig. 5. A 4-node rectangular shell element is used to model the steel structure with each node having 6 degrees of freedom (three translations and three rotations).

The solid element is also used to model the behavior of the RPF layer. The solid element is chosen since it possesses in-plane and out-of-plane stiffnesses. The solid element allows for both in-plane and out-of-plane loads. The solid element is cubic in shape and has 8 nodes each having 3 degrees of freedom (three translations).

The mechanical properties of the sandwich steel structure are Poisson's ratio v=0.3; averaged mass density of steel 7900 kg/m^3; elastic modulus E= 2350 t/cm^2; and yield strength f_y= 3500 kg/cm^2. The shear modulus of the steel depends on the elastic modulus (E) and Poisson's ratio (v).

The mechanical properties of the RPF layer are Poisson's ratio $\nu = 0.3$; averaged mass density of RPF layer 120 kg/m^3; bulk modulus of RPF E_i= 20 t/cm^2; and yield strength f_y= 350 kg/cm^2. The shear modulus of the RPF depends on the elastic modulus (E) and Poisson's ratio (v).

The cubic solid element and the rectangular shell element interface are used between the RPF layer and the sandwich steel structure to ensure the compatibility conditions at the interface surface between them as well as the associated stresses and strains along the interface surface. This type of finite element is used to link adjacent nodes characterized by stiffness components.

3. Blast field test

In this study, field blast test is conducted to understand the sandwich steel structure performance based on different TNT explosive charges and the RPF. Two models of XCS steel structure and CSS steel structure are also prepared and tested in this study. The dimensions for each hexagonal tube (1 mm thickness) of this internal core structure system in the sandwich steel structure are shown in Fig. 2. The dimensions for each channel stiffener (2 mm thickness) of this internal core structure system in the sandwich steel structure are also shown in Fig. 3. In addition, the outer covers of the sandwich steel structure are steel plates. The steel plates are square in shape of 1.0 m height, 1.0 m width, and 6 mm thickness, as shown in Fig. 5. The interior spacing (core spacing) between the steel plates of the sandwich steel structure is 10 cm. The thickness of the RPF layer covering the sandwich steel structure is 10 cm with the same core spacing of the sandwich steel structure, as shown in Figs. 2 and 4.

The XCS structure without the RPF is subjected to 1-kg, 2-kg, and 3-kg TNT explosive charges, as shown in Fig. 2. The XCS structure strengthened by the RPF is also prepared and

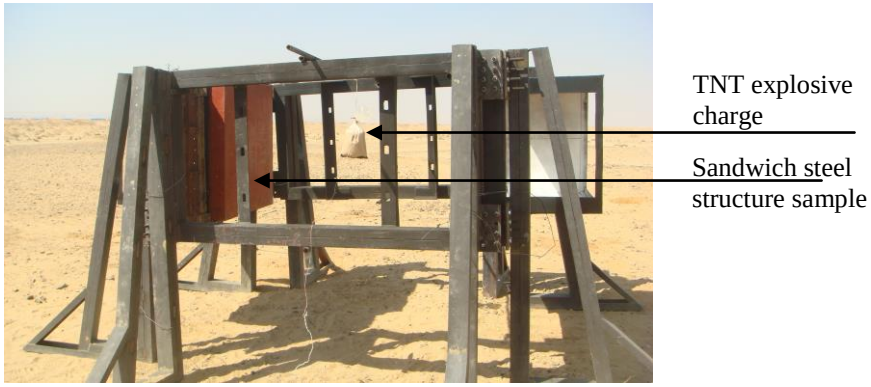

Fig. 6 Test rig

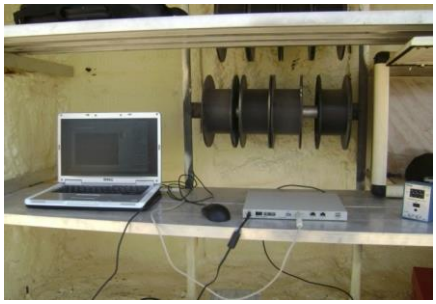

Field instrumentation devices

Measurement sensors

Fig. 7 Field blast system measurement devices

tested under different TNT explosive charges. The CSS structure without the RPF is subjected to 1-kg TNT, 2-kg TNT, and 3-kg TNT explosive charges, as shown in Fig. 3. The CCS structure strengthened by the RPF is also tested under different TNT explosive charges.

The previous specimens are prepared and assembled with special requirements to be tested against TNT explosives. A test rig is prepared and used to simulate the sandwich steel structure boundary in free air. However, the test rig also needs some precautions to satisfy boundary conditions for free air explosion. The dimension of the test rig is 2 m × 2 m × 2 m, as shown in Fig. 6. The members of the test rig are box sections composed from two channel 140 mm. These box members are welded face to face. Angles (70 mm × 7 mm) are also welded to the box members in vertical and horizontal directions so as to support the test models, as shown in 6. The height of the supporting angles is 1.0 m and their width is 1.0 m, as shown in Fig. 6.

The sensor interface PCD-30A is a voltagemeter that is connected with the personal computer so as to record pressure-time history hitting the sandwich steel structure due to blast effect. The maximum displacements of the specimens are also measured under blast loading. LVDTs are placed at the centre of the sandwich steel door. The sensors are used to record maximum displacement at the centre of the sandwich steel door, as shown in Fig. 5. This device is capable of measuring voltage which is recorded and attached to control software. This system can measure four channels. The sensors are also attached on the center of the specimen's top surface. The locations of the attached sensors are shown in Fig. 5 (point 1). Fig. 7 shows the field instrumentation devices.

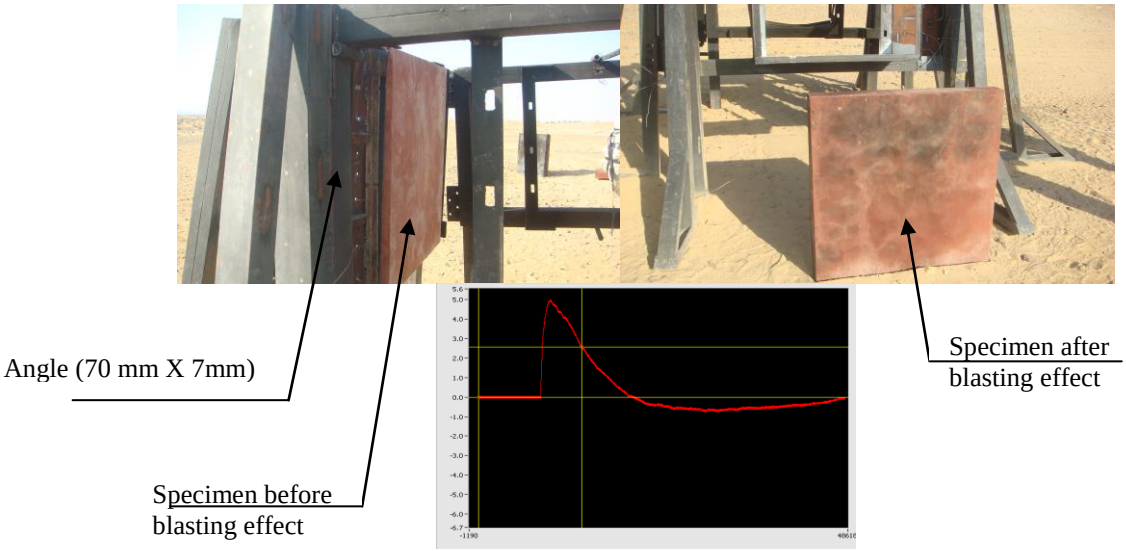

Fig. 8 Hexagonal core sandwich steel structure (XCS) subjected to 2-kg TNT explosive charge

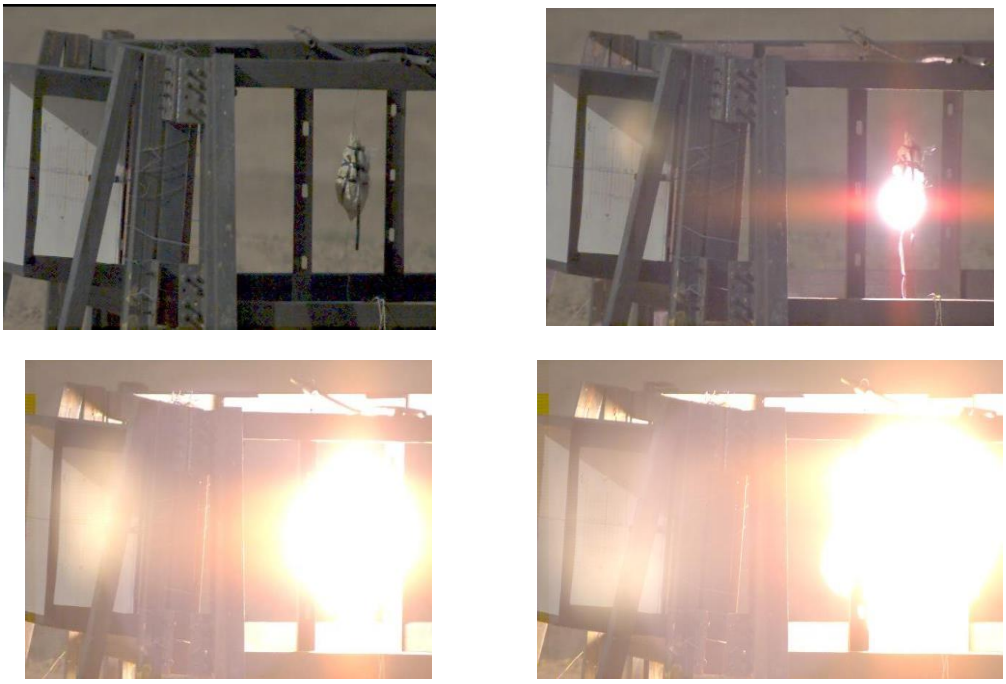

Fig. 9 Explosive scene by 2-kg TNT explosive

The XCS structure and the CCS structure are subjected to blast pressure recorded at the case of 2-kg TNT explosive charge, as shown in Fig. 8. The high speed camera is also used to capture photos at 15000- 20000 frames/s. The photos of explosion with TNT charge of 2 kg are shown in Fig. 9.

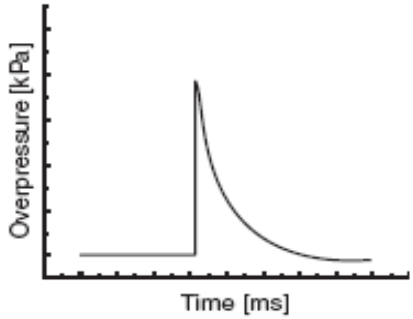

Fig. 10 Typical pressure time history in open air (after Gaissmaire 2003)

4. Numerical model verification

The shock of the blast wave is generated when the surrounding atmosphere is subjected to an extreme compressive pulse radiating outward from the centre of the TNT explosive. The pressure–time history of a blast wave is illustrated with a general shape by Gaissmaire (2003), as shown in Fig. 10. The illustration is an idealization for an explosion in free air, as shown in Fig. 10. Transient pressure being greater than ambient pressure is defined as the overpressure (P_s) (Smith and Hetherington 1994). The peak overpressure (P_s) is the maximum value of the overpressure at a given location. The rise time to peak overpressure is less than microsecond (Baker *et al*. 1983).

This study presents a comparison between the pressure-time histories obtained by the empirical method (EM) developed by Henrych (Beshara 1994), by the field blast test, and by the numerical model. The EM method uses the stand-off distance (R) to calculate the scaled distance (Z) and the peak overpressure as presented in Eq. (1) (Beshara 1994).

$$Z = \frac{R}{\sqrt[3]{W}} \tag{1}$$

Where; R is the stand-off distance from the centre of the explosion to a given location in meter and W is the weight of the explosive in kg.

The equations developed by Henrych (Beshara 1994) divide the analysis into three fields based on scaled distances (Z) as presented in Eqs. (2) to (4).

$$P_s = \frac{14.072}{Z} + \frac{5.540}{Z^2} - \frac{0.357}{Z^3} + \frac{0.00625}{Z^4} \ (bar) \qquad \text{(for } 0.05 < Z < 0.3\text{)} \tag{2}$$

$$P_s = \frac{6.194}{Z} - \frac{0.326}{Z^2} + \frac{2.132}{Z^3} (bar) \qquad \text{(for } 0.3 < Z < 1\text{)} \tag{3}$$

$$P_s = \frac{0.662}{Z} + \frac{4.05}{Z^2} + \frac{3.288}{Z^3} \ (bar) \qquad \text{(for } 1 < Z < 10\text{)} \tag{4}$$

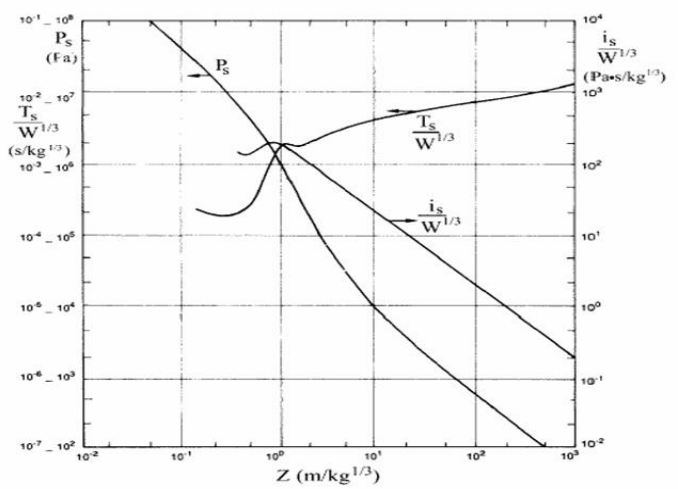

Fig. 11 Blast wave parameters for spherical charges of TNT (after Smith and Hetherington 1994)

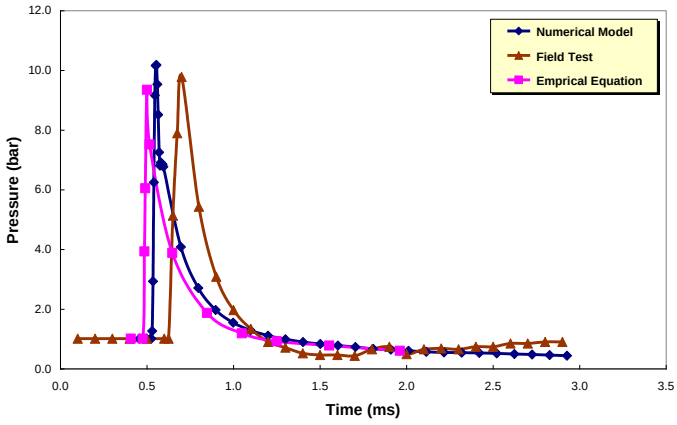

Fig. 12 Pressure-time history hitting sandwich steel structure at point 1 for 1-kg TNT explosive

The scaled distance (Z) is also used to determine the positive duration time (T_s) and the positive impulse (i_s) by using Fig. 11 (Smith and Hetherington 1994).

This study is also extended to assess the accuracy of the numerical model. One-kg TNT, two-kg TNT, and three-kg TNT explosives are applied at stand-off distance (R) of one meter to obtain the pressure-time history hitting the sandwich steel structure by the EM, the numerical model, and the field blast test at points 1 and 2 (Fig. 5), as shown in Figs. 12 to 14. The result shows that the pressure-time histories obtained by the field blast test agree well with those estimated by the numerical model and the EM.

5. Blast impact on performance of sandwich structure strengthened by RPF layer

The displacement-time history hitting the XCS steel structure and the CSS steel structure due to

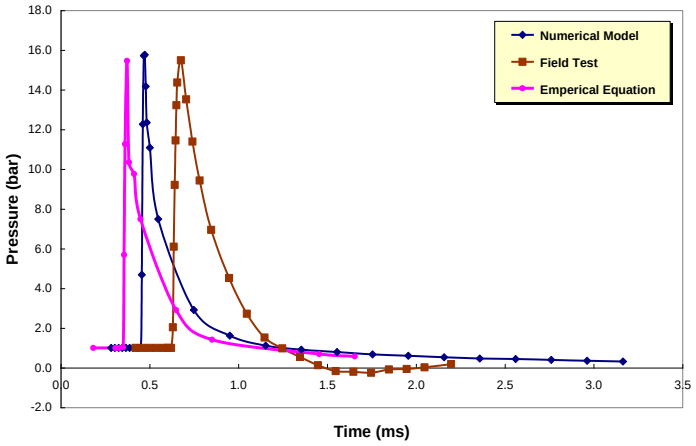

Fig. 13 Pressure-time history hitting sandwich steel structure at point 1 for 2-kg TNT explosive

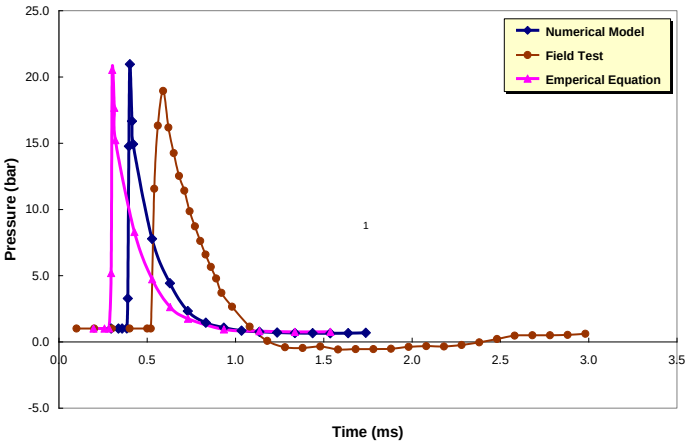

Fig. 14 Pressure-time history hitting sandwich steel structure at point 1 for 3-kg TNT explosive

centre of the sandwich steel blast load is calculated using the 3-D numerical model. The maximum displacements at the structure obtained by the FEA are compared with those obtained by the field blast test. The FEA is used to calculate the displacement-time history of the sandwich steel structure strengthened by the RPF layer as mitigation system. The study discusses the impact of the RPF layer on the sandwich steel structure performance under blast impact.

Four cases of the sandwich steel structure with and without the RPF layer are studied. At the first case, the XCS structure is modeled without the RPF layer. At the second case, the CSS structure is modeled without the RPF layer. At the third case, the XCS structure is modeled using the RPF layer. At the fourth case, the CSS structure is modeled using the RPF layer.

One-kg TNT explosive is used to discuss the impact of the RPF layer on both the XCS structure and the CSS structure at points 1 and 2 (Fig. 5). The TNT explosive is located at one-meter stand-off distance from the samples, as shown in Fig. 4. The pressure- time history hitting the steel structure is presented in Fig. 12. The displacement-time history profiles at points 1 and 2

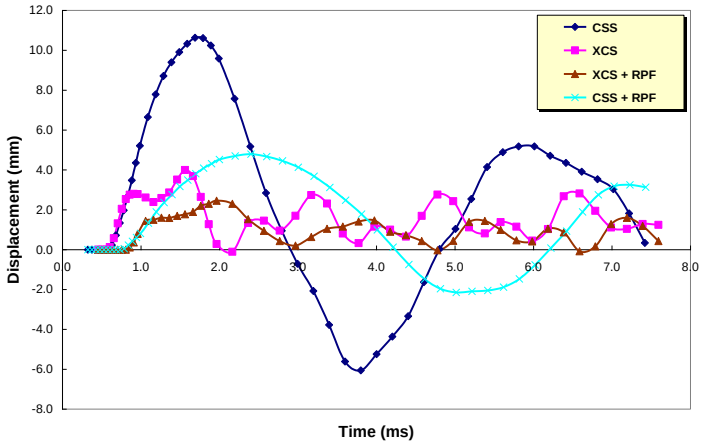

Fig. 15 Displacement–time history of sandwich steel structure at point 1 (1 kg TNT)

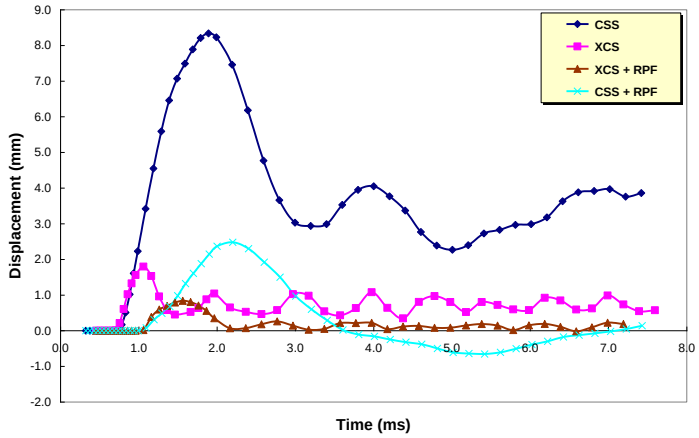

Fig. 16 Displacement–time history of sandwich steel structure at point 2 (1 kg TNT)

at the XCS structure and the CSS structure for the four cases are calculated to discuss the impact of the RPF layer. Fig. 15 shows the comparison between the displacement-time histories at point 1 for each case. Fig. 16 also presents the comparison between the displacement-time histories at point 2 for each case. The maximum displacements at the centre of the XCS steel structure and the CSS steel structure obtained by the FEA are compared with those obtained by the field blast test as tabulated in Table 1. The comparison also indicates that the response of the sandwich steel structures strengthened by the RPF layer is the smallest response with respect to the response of the sandwich steel structures without the RPF layer.

Two-kg TNT explosive is also used to discuss the impact of the RPF layer on both the XCS structure and the CSS structure at points 1 and 2 (Fig. 5). The pressure- time history hitting the steel structure is also presented in Fig. 13. The displacement-time history profiles at points 1 and 2 at the XCS structure and the CSS structure for the four cases are calculated to discuss the impact of the RPF layer. Fig. 17 shows the comparison between the displacement-time histories at point 1 for each case. Fig. 18 also presents the comparison between the displacement-time histories at

Table 1 Maximum displacement at the centre of the sandwich steel structures (point 1) under different TNT explosives

Sample	TNT explosive (kg)	Maximum recorded displacement (mm)	Maximum computed displacement (mm)
XCS structure without RPF	1	4.4	4
	2	7.8	7.2
	3	10.5	9.8
XCS structure strengthened by RPF	1	2.6	2.3
	2	5.3	4.8
	3	8.9	8.1
CSS structure without RPF	1	11.9	10.8
	2	16.5	15.4
	3	21.1	19.8
CSS structure strengthened by RPF	1	5.3	4.8
	2	8.4	7.7
	3	11.8	10.9

Note: XCS is hexagonal core sandwich structure (XCS) and CSS is channel stiffener sandwich structure (CSS).

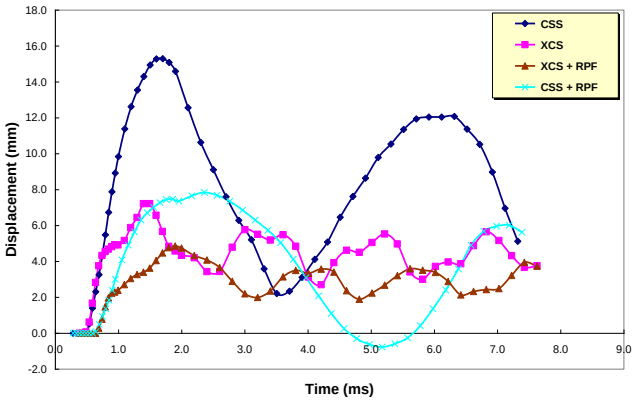

Fig. 17 Displacement–time history of sandwich steel structure at point 1 (2 kg TNT)

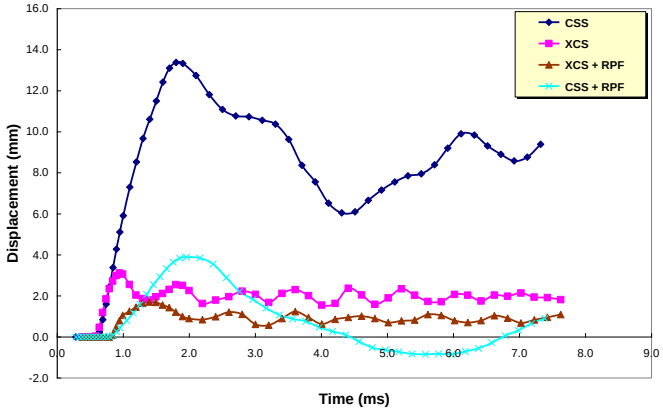

Fig. 18 Displacement–time history sandwich steel structure at point 2 (2 kg TNT)

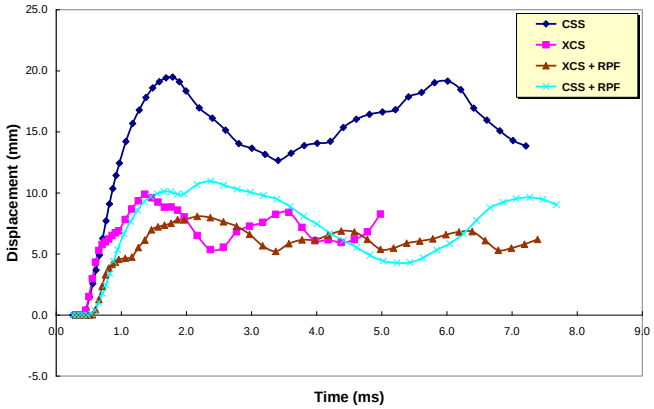

Fig. 19 Displacement–time history of sandwich steel structure at point 1 (3 kg TNT)

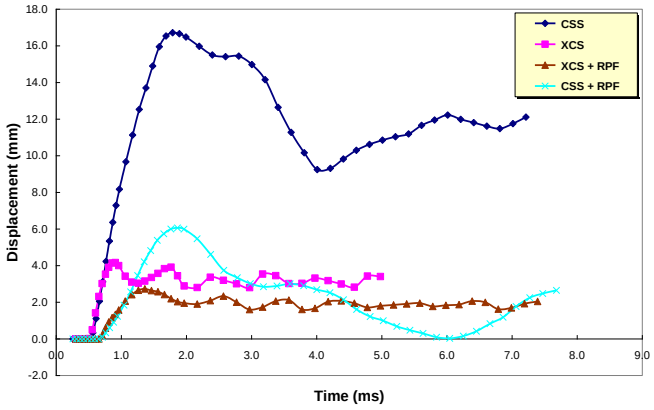

Fig. 20 Displacement–time history of sandwich steel structure at point 2 (3 kg TNT)

point 2 for each case. The maximum displacements at the centre of the XCS steel structure and the CSS steel structure obtained by the FEA are also compared with those obtained by the field blast test as written in Table 1. The comparison shows that the response of the sandwich steel structures strengthened by the RPF layer is the smallest response with respect to the response of the sandwich steel structures without the RPF layer.

Three-kg TNT explosive is used to discuss the impact of the RPF layer on both the XCS structure and the CSS structure at points 1 and 2 (Fig. 5). The results demonstrate that the response of the sandwich steel structures strengthened by the RPF layer is again the smallest response with respect to the response of the sandwich steel structures without the RPF layer as shown in Figs. 19 and 20 and as presented in Table 1.

6. Discussions

The difference between the performance of the sandwich steel structures with and without the RPF layer lies in the use of the RPF layer. The XCS and the CSS structures (Figs. 2 and 3) are

used to discuss the impact of the RPF layer on the performance of the steel structures.

The field blast test is conducted to study the performance of the XCS and the CSS structures strengthened by the RPF layer and to trace the pressure-time histories hitting the sandwich panel based on different TNT explosive charges. The pressure-time history hitting the sandwich structures and the maximum displacement of the sandwich structures are recorded and computed. The trends of the pressure-time histories obtained by the field blast test, the numerical model, and the empirical method are the same trend as those presented by Gaissmaire (2003). There is a good agreement between the pressure-time histories obtained by the field blast test and the numerical model.

The FEA also gives a better estimation of the response of the sandwich steel structures with and without the RPF layer as tabulated in Table 1 based on different the TNT explosive charges. There is also a good agreement between the recoded and the computed maximum displacements of the sandwich structures.

In general, the sandwich steel structures play an important role to resist the blast load. The case of the sandwich steel structures strengthened by the RPF layer gives the smallest displacement readings. Therefore, the RPF layer increases the steel structure stiffness and then reduces the deformation of the sandwich steel structure compared to the sandwich steel structure without the RPF layer. The RPF has a large amount of strain energy which can absorb the kinetic energy of the blast wave propagation. Based on the field blast test and the FEA, the RPF reduces the maximum displacement of the XCS structure up to 30%. The RPF reduces the maximum displacement of the CSS structure up to 50%. Finally, the performance of the sandwich steel structures is highly dependent on the material properties of the RPF layer which is used as a mitigation system.

7. Conclusions

A 3-D nonlinear finite element analysis has been used to predict the performance of sandwich steel structures with and without PRF layers under the blast effect. In this study, the performance of the sandwich steel structures with and without the RPF layer is modeled and analyzed using nonlinear finite element computer program Autodyn3D (2005). The field blast test is also conducted. The following conclusions can be drawn regarding the performance of the sandwich steel structures strengthened by the RPF layer under impact of shock wave propagation.

• Based on the field blast test and the empirical method developed by Henrych (Beshara 1994), the 3-D numerical model gives a better estimate of the pressure-time history hitting the sandwich steel structure.

• The pressure-time histories calculated by the 3-D numerical model is in reasonable agreement with those obtained by both the field blast test the empirical method developed by Henrych (Beshara 1994).

• The pressure-time history profile of the sandwich steel panel calculated by the numerical model has the same trend as that presented by Gaissmaire (2003).

• The 3-D finite element model can be successfully used to analyze and estimate the performance of the sandwich steel panels with and without the PCS layers based on the field blast test.

• The response of the XCS steel structure strengthened by the RPF layer is reduced up to 30% with respect to that of the XCS steel structure without the RPF layer.

• The response of the CSS steel structure strengthened by the RPF layer is reduced up to 50%

with respect to that of the CSS steel structure without the RPF layer.

However, the rigid polyurethane foam (RPF) layer could be used as structural retrofitting to absorb the energy of the blast wave propagation hitting the sandwich steel structures.

References

Aimone, C.T. (1982), "Three-dimensional wave propagation model of full-scale rock fragmentation, Ph.D. Thesis, Northwestern University.

AUTODYN (2005), "Theory Manuals", Version 6.1, Century Dynamics Inc., Sam Ramon, USA.

Baker, W.E., Cox, P.A., Kulesz, J.J. and Strehlow, R.A. (1983), *Explosion Hazards and Evaluation*, Elsevier.

Beshara, F.B.A. (1994), "Modeling of blast loading on aboveground structures -I. Internal blast and ground shock", *Comp. Struct*., **51**(3), 585-596.

Chen, H. and Chen, S. (1996), "Dynamic responses of shallow-buried flexible plates subjected to impact loading", *Journal of Structure Engineering*, **122**(1), 55-60.

Dharmasena, K.P., Wadley, H.N., Xue, Z. and Hutchinson, J.W. (2008), "Mechanical response of metallic honeycomb sandwich panel structures to high-intensity dynamic loading", *International Journal of Impact Engineering*, **35**(9), 1063-1074.

Fayad, H.M. (2009), "The optimum design of the tunnels armoured doors under blast effects", Ph.D. Thesis, Military Technical College (MTC), Cairo.

Gaissmaiere, A.E.W. (2003), "Aspects of thermobaric weapon", *ADF Health*, **4**, 3-6.

Gustafsson, R. (1973), *Swedish Blasting Technique*, Gothenburg, Sweden, SPI.

Ha, J., Yi, N., Choi, J. and Kim, J. (2011), "Experimental study on hybrid CFRP-PU strengthening effect on RC panels under blast loading", Journal of Composite Structures, **93**, 2070-2082.

Hao, H., Ma, G.W. and Zhou, Y.X. (1998), "Numerical simulation of underground explosions", *Fragblast Int. J. Blasting and Fragmentation*, **2**, 383-395.

Liu, L. and Katsabanis, P.D. (1997), "Development of a continuum damage model for blasting analysis", *Int. J. Rock Mech. Min. Sci*., **34**, 217-231.

Lu, Y., Wang, Z. and Chong, K. (2005), "A comparative study of buried structure in soil subjected to blast load using 2-D and 3-D numerical simulations", *Journal Soil Dynamics and Earthquake Engineering*, **25**, 275-288.

Luccioni, B., Ambrosini, D., Nurick, G. and Snyman, I. (2009), "Craters produced by underground explosions", *Journal of Computers and Structures*, **87**, 1366- 1373.

Mohamad, L.S. (2006), "Study and design of fortified structures due to blast effects", M.Sc Thesis, Military Technical College (MTC), Cairo, Ammunition and Explosives, AC/258-D/258, Brussels, Belgium.

Remennikov, A. (2003), "A review of methods for predicting bomb blast effects on buildings", *Journal of Battlefield Technology*, **6**(3), 155- 161.

Schueller, C.T. (1991), *Structural Dynamics*, Springer-Verlag, Berlin, New York.

Smith, P.D. and Hetherington, J.G. (1994), *Blast and Ballistic Loading of Structures*, Butterworth-Heinemann Ltd., UK.

Technical Manual TM 5-885-1 (1986), Fundamentals of Protective Design for Conventional Weapons, Headquarters Department of the Army, Washington DC.

Technical Manual TM 5-1300 (2008), Structures to Resist the Effects of Accidental Explotions, Unified Facilities Criteria (UFC), U.S. Army Corps of Engineers, Naval Facilities Engineering Command, Air Force Civil Engineer Support Agency.

Trelat, S., Sochet, I., Autrusson, B., Cheval, K. and Loiseau, O. (2007), Impact of a shock wave on a structure on explosion at altitude, Journal of Loss Prevention on the Process Industries, **20**, 509-516.

Wu, C., Hao, H. and Zhou, Y.X. (1999), "Dynamic response analysis of rock mass with stochastic properties subjected to explosive loads", *Fragblast the International J. Blasting and Fragmentation*, **3**, 137-153.

Zhang, W. and Valliappan, S. (1990), "Analysis of random anisotropic damage mechanics problems of rock mass, Part II: statistical estimation", *Rock Mechanics and Rock Engineering*, **23**, 241-259.